Digital Microfluidic Cell Culture

Alphonsus H.C. Ng,[1,2] Bingyu Betty Li,[1,2] M. Dean Chamberlain,[1,2] and Aaron R. Wheeler[1,2,3]

[1]Institute for Biomaterials and Biomedical Engineering, University of Toronto, Toronto, Ontario M5S 3G9, Canada; email: aaron.wheeler@utoronto.ca

[2]The Terrence Donnelly Center for Cellular and Biomolecular Research, Toronto, Ontario M5S 3E1, Canada

[3]Department of Chemistry, University of Toronto, Toronto, Ontario M5S 3H6, Canada

Annu. Rev. Biomed. Eng. 2015. 17:91–112

The *Annual Review of Biomedical Engineering* is online at bioeng.annualreviews.org

This article's doi: 10.1146/annurev-bioeng-071114-040808

Keywords

droplet, electrowetting on dielectric, hydrogel, drug screening, protein adsorption, organ-on-a-chip

Abstract

Digital microfluidics (DMF) is a droplet-based liquid-handling technology that has recently become popular for cell culture and analysis. In DMF, picoliter- to microliter-sized droplets are manipulated on a planar surface using electric fields, thus enabling software-reconfigurable operations on individual droplets, such as move, merge, split, and dispense from reservoirs. Using this technique, multistep cell-based processes can be carried out using simple and compact instrumentation, making DMF an attractive platform for eventual integration into routine biology workflows. In this review, we summarize the state-of-the-art in DMF cell culture, and describe design considerations, types of DMF cell culture, and cell-based applications of DMF.

Contents

1. INTRODUCTION

The increasing demands of biological research and drug discovery have led to the development of liquid-handling robotics that can be used for automated cell culture and analysis (1). These systems solve two problems: (*a*) They enable a massive increase in parallel analyses for high-throughput applications, and (*b*) they offer relief from the tedium of the never-ending steps required to culture cells (seed, feed, wash, passage, repeat, etc.). But robotic liquid handlers are not a panacea for all applications, and, in fact, the high capital costs, large volumes of reagent consumed, and high turnover of consumables make them cost-prohibitive in many settings. This is problematic even in the pharmaceutical industry, which is currently facing significant challenges related to the unsustainable costs of research and development (2, 3). This is one motivation for the development of microfluidic cell-culture platforms that have the capability to manipulate fluids at the nanoliter scale (4, 5). Although most microfluidic methods cannot match the throughput of robotic handlers, they certainly hold promise for providing relief from the tedium of processing. The past two decades have seen the development of a wide range of diverse microfluidic technologies, including continuous fluid flow in enclosed microchannels, immiscible droplets manipulated in enclosed microchannels, and the digital microfluidic manipulation of droplets on planar surfaces. Each of these formats has its own advantages and disadvantages (6); here we focus on digital microfluidics (DMF) (7, 8), which has only recently become popular for cell culture and analysis.

In DMF, samples and reagents are manipulated as discrete picoliter- to microliter-sized droplets on a hydrophobic surface. The most common DMF systems actuate droplets through the application of electrical potentials on a generic ($m \times n$) array of insulated electrodes (**Figure 1*a***). The generic geometry and simple actuation scheme allow users to adopt a programming approach to microfluidics, calling a series of functions comprising various combinations of metering from reservoirs, splitting, merging, and mixing (**Figure 1*b–d***) in any number or order. There are also alternative electrode-less DMF actuation modalities that are driven by optical, magnetic, thermocapillary, and surface acoustic-wave forces (8), but the focus here is on the most common format—that is, devices relying on electrostatic forces to move droplets on arrays of electrodes.

Like the microfluidic formats that rely on microchannels, DMF benefits from small fluid volumes, the rapid transfer of heat and gas, a high capacity for parallelization and automation, and

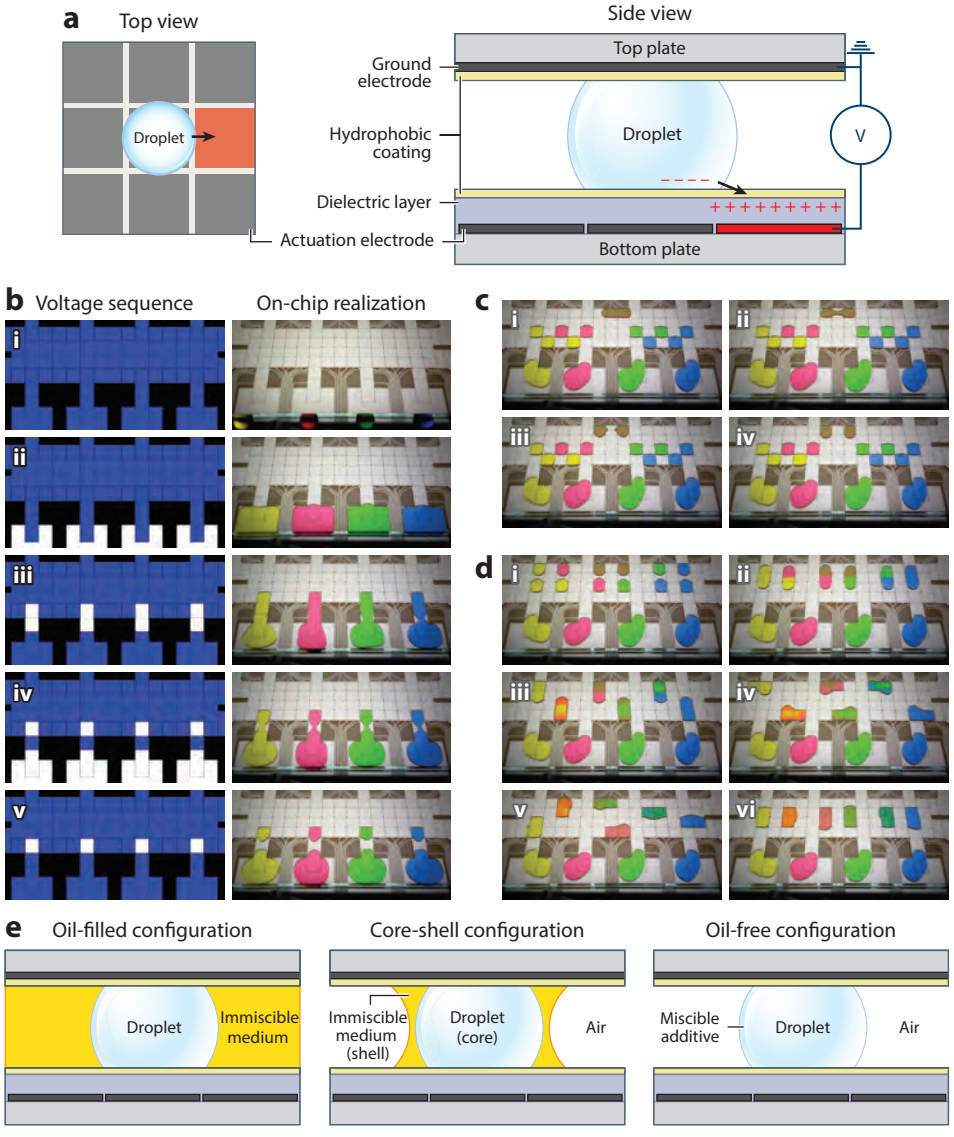

Figure 1

Digital microfluidics (DMF). (*a*, *left*) Top view and (*right*) side view schematics of a two-plate DMF device. (*b*, *left*) Graphical representation of a preprogrammed voltage sequence and (*right*) corresponding frames from a video depicting the metering of droplets from reservoirs. Frames from videos depicting (*c*) the splitting of a droplet and (*d*) the merging and mixing of droplets. Dyes were added to the droplets to enhance visibility. (*e*) Methods for preventing protein adsorption include (*left*) the oil-filled configuration, (*middle*) the core-shell configuration, and (*right*) the oil-free configuration with miscible additive.

straightforward integration with existing analytical techniques (9). However, unlike channel-based formats, fluid manipulation in DMF does not require networks of channels, pumps, valves, or mechanical mixers. Thus, elaborate multistep applications involving cells can be performed with simple and compact instrumentation, making it an attractive platform for eventual integration into routine biology workflows. In this review, we summarize the state-of-the-art in DMF cell culture, and focus particularly on DMF design considerations, types of DMF cell culture, and DMF cell-based applications.

2. DESIGN CONSIDERATIONS

Various techniques have been developed to make DMF compatible with techniques for culturing cells and small organisms. In this section, we discuss methods for preventing protein adsorption and ensuring biocompatibility of device and on-chip reagents.

2.1. Preventing Protein Adsorption

The most versatile and prevalent format for DMF devices is the two-plate configuration, in which droplets are sandwiched between two parallel substrates patterned with electrodes (**Figure 1*a***). Typically, the bottom plate houses an array of actuation electrodes (of any conductive material) covered by an insulating dielectric layer [e.g., parylene C, silicon nitride, polydimethylsiloxane (PDMS), or SU-8]. These electrodes are referenced to a continuous ground electrode in the top plate made from indium tin oxide (ITO), an optically transparent conductive material. Spacers are used to separate the top and bottom plates, resulting in a fixed gap between them. Critically, both plates are coated with a fluorinated hydrophobic coating [e.g., Teflon AF (DuPont, Wilmington, DE), Cytop (Asahi Glass, Tokyo, Japan), or FluoroPel (Cytonix, Beltsville, MD)] to minimize the friction experienced by aqueous droplets during actuation. By applying a sequence of pre-programmed voltages (**Figure 1*b***), this configuration affords a wide range of droplet operations, including metering droplets from reservoirs, splitting (**Figure 1*c***), merging (**Figure 1*d***), and mixing (10). Unfortunately, the necessity of using a hydrophobic layer makes it challenging to move droplets that contain proteins. When proteins in aqueous solution encounter a hydrophobic solid surface, it is often thermodynamically favorable for the proteins to become immobilized on the surface via hydrophobic interactions (11, 12). As such, any contact between the liquid droplet and the hydrophobic surface will promote protein adsorption, causing the surface to become hydrophilic. When this happens to a sufficient degree, droplet transport is impeded. For example, the maximum movable concentration of bovine serum albumin (BSA) in a two-plate device (operated in air) is a mere 0.005 mg/mL (13, 14). This low concentration is not adequate for most cell-culture applications, which often require growth media containing protein concentrations that are at least 3 orders of magnitude higher (i.e., 5 mg/mL or greater). To enable transport of increased concentrations of proteins (up to 10 mg/mL BSA), Freire & Tanner (15) developed a device with modified geometry that pulls the droplet away from the surface. This field-dewetting configuration does not support all of the essential fluidic operations, such as droplet splitting or metering droplets from reservoirs (10), but it may be useful for some simple cell-based applications.

To operate DMF devices without sacrificing the capability to perform essential droplet operations, the two most effective techniques used to prevent protein adsorption involve (*a*) encapsulating droplets in a nonconductive, immiscible liquid, or (*b*) doping additives into the aqueous droplets themselves. In the first method, devices are filled with a low-viscosity fluid (typically silicone oil); in this configuration (**Figure 1*e***, *left*), droplets (which must be immiscible with the

filler) are encapsulated by a film, which prevents them from directly contacting the hydrophobic surface. Using this approach, Srinivasan et al. (16) demonstrated successful manipulation of various protein-rich droplets from physiological sources, including whole blood, serum, plasma, urine, saliva, sweat, and tears. In general, the stability of the oil film around each droplet decreases with increasing protein concentration because of the decrease in liquid–oil interfacial tension. To enhance the stability of the oil film, a lipophilic surfactant such as Triton X-15 (Dow Chemical, Midland, MI) can be added to the oil to further decrease its surface tension, and, therefore, increase the liquid–oil interfacial tension. Pollack et al. (17) demonstrated that this strategy enables reliable manipulation of droplets containing up to 75 mg/mL of lysozyme. In addition to preventing protein adsorption, the oil-filled configuration has many other advantages, including low actuation voltage and minimal droplet evaporation (which is particularly useful for applications requiring high temperatures, e.g., polymerase chain reaction). Conversely, the presence of oil imposes a viscous drag on the droplet, which can increase the power required (18) and limit the speed of droplet movement. Indeed, if a droplet moves too fast through the oil phase, the droplet may inadvertently split or fragment. To address these and other limitations, Bassard et al. (19) developed a hybrid technique, in which aqueous droplets are encapsulated in a thin oil shell and transported on a device that is predominantly filled with air (**Figure 1*e***, *middle*). This aqueous–oil core-shell configuration supports all fundamental droplet operations while lowering viscous drag and eliminating the fabrication and packaging required to confine a large pool of silicone oil in the device. Because of its low volatility, silicone-oil fillers may be incompatible with applications that require in situ drying of droplets (e.g., to isolate proteins for crystallization experiments or for dissolution in a different solvent). To circumvent this problem, Fan et al. (20) developed a technique to remove the oil in a core-shell droplet by bringing the droplet into a reservoir of hexane. After the oil has been dissolved in hexane, the droplet is moved out of the reservoir and the remnant hexane is rapidly evaporated, leaving behind the bare aqueous droplet. As an alternative, Aijian et al. (21) used fluorinated fluids (instead of silicone oil) to generate the core-shell droplet configuration. Because fluorinated liquids are predominantly immiscible with aqueous (and organic) solvents and are relatively volatile, they can facilitate droplet movement and subsequently be removed by evaporation at room temperature, enabling users to deliberately dry or crystallize samples as needed.

In the second class of techniques, an additive is included in the droplet composition to prevent proteins from interacting with the surface (**Figure 1*e***, *right*). For example, Perry et al. (22, 23) used graphene oxide (GO) additives to enable the movement of droplets containing up to 0.26 mg/mL of BSA in oil-free devices. The GO molecules act as nanosponges for proteins: If the concentration of GO is at least double that of BSA, then there will be sufficient GO to bind the proteins in solution, thus preventing them from adsorbing onto the device's surface. However, there is no indication whether proteins can be released from GO after transport. The most well-established additive for preventing protein adsorption in DMF is Pluronic (BASF, Ludwigshafen, Germany). This family of triblock copolymers is formed from a relatively hydrophobic poly(propylene oxide) (PPO) chain flanked by two relatively hydrophilic poly(ethylene oxide) (PEO) chains (PEO-PPO-PEO). Amphiphilic molecules (bearing both hydrophobic and hydrophilic residues) are known to reduce protein and cell adsorption to hydrophobic surfaces; in the many different varieties of Pluronic, this property is tuned by varying the lengths of the PPO and PEO components (24). Adding low concentrations (0.08%) of Pluronic F127 (with PEO-PPO-PEO average chain length of 100/65/100), Luk et al. (13) demonstrated movement of droplets containing up to 50 mg/mL of BSA in oil-free devices. In a more systematic study, Au et al. (25) tested a series of eight Pluronic surfactants using cell-culture media containing 10% bovine serum as a model fluid. Consistent with previous observations (24), the authors observed that Pluronics with longer hydrophobic

PPO chains are better at reducing protein adsorption during droplet movement. Specifically, Pluronics with fewer than 30 PPO units (F38, L35, and L44) fail to enable the translation of droplets containing 10% fetal bovine serum, but Pluronics with more than 30 PPO units (F68, L64, L62, L92, and P105) support movement for hundreds of droplet operations.

To exploit the benefits of multiple approaches, some groups have implemented more than one technique in a device. For example, Vergauwe et al. (26) and Li et al. (27) employed both an oil core-shell configuration and Pluronic additives to culture, respectively, cells and embryos. Similarly, Sarvothaman et al. (28) combined Pluronic additives with a new type of amphiphilic, fluorinated device coating to facilitate extremely long-lived cell culture media droplet manipulation. The choice of method (or methods) used for preventing protein adsorption depends on the application and the biocompatibility of the approach (as described in Section 2.2).

2.2. Biocompatibility

As is the case for other, more established in vitro culture systems, in order for DMF to be useful, it must be biocompatible with the cells and organisms being studied. In particular, the methods for preventing protein adsorption (described in Section 2.1), and the electrical and mechanical effects of the droplet actuation process must have negligible effects on cell and organism phenotype.

As described in Section 2.1, preventing protein adsorption requires the use of reagent additives that are water soluble (Pluronics and graphene oxide) or filler fluids that are immiscible (fluorinated liquids and silicone oils). Ideally, the effects of these reagents on cell health should be evaluated in a well plate (or other non-DMF) format so that the potential cytotoxicity of each reagent can be decoupled from the effects of droplet manipulation. A major question about water-soluble additives is whether they have the potential to interact with cells, which could be toxic or cause unintentional cellular stimulation or inhibition. Pluronics are known to be particularly gentle additives, and some commercial, mammalian-cell media formulations include Pluronics as a constituent (29). But not all Pluronics are biocompatible; Au et al. (25) investigated the effects of culturing Chinese hamster ovary (CHO) cells in well plates in the presence of five Pluronic species that have at least 30 PPO units (which is required for droplet movement). Interestingly, the authors found that the nontoxic Pluronic species (F68 and P105) had at least 50% PEO content, and, therefore, had higher values of hydrophilic–lipophilic balance (HLB) compared with their toxic counterparts (L62, L64, and L92). The authors speculated that the Pluronics with lower HLB values, which were found to be toxic, are more likely to interact with phospholipid bilayers, and, thereby, disrupt the integrity of the cell membrane. From these observations, the authors postulated that Pluronics with high PEO content and long PPO chain lengths, such as F88 and F108 (not tested in the original study), would also be good candidates for DMF cell-based assays. In later work, the same authors (30) demonstrated that F88 is indeed suitable for coculture of hepatocyte and fibroblast cell lines in a DMF system. **Table 1** summarizes the properties of various Pluronic additives and the empirical reports of their suitability for culture-media transport, cell culture, or both. The alternative to Pluronic additives, GO, is likely incompatible with applications involving cells. In a recent study, Wang et al. (31) found that GO is toxic to human fibroblasts. For example, if more than 50 μg/mL of GO is cultured with human fibroblasts, the cells exhibit cytotoxic phenotypes, including a decrease in cell adhesion and the induction of apoptosis. Because a ratio of GO to BSA greater than 2 is required for droplet movement (22), the GO concentration required to move cell media is at least 200 times higher than a toxic dose.

The alternative to using solution additives to reduce biofouling is to use immiscible filler fluids. Since the filler does not interact with the cells directly, two different problems for cell culture may arise (32): (*a*) the encapsulation of a droplet may restrict gas exchange, and (*b*) proteins and

Table 1 Properties of different species of Pluronics (BASF, Ludwigshafen, Germany) (PEO_m-PPO_n-PEO_m) tested as droplet additives for preventing protein adsorption in digital microfluidic devices

Pluronic	Average molecular weight	Average PPO length (n)	Average PEO length (m)	PEO content (%)	HLB	Suitable for media transport	Suitable for cell culture	Reference(s)
L35	1,900	16	11	50	18–23	No	Not tested	25
F38	4,700	16	46	80	>24	No	Not tested	25
L44	2,200	21	11	40	12–18	No	Not tested	25
L62	2,500	30	8	20	1–7	Yes	No	25
L64	2,900	30	13	40	12–18	Yes	No	25
F68	8,400	30	75	80	>24	Yes	Yes	39, 42–46, 49, 51, 55, 57, 63, 64, 66, 69, 70
L92	3,650	47	10	20	1–7	Yes	No	25
P105	6,500	56	37	50	12–18	Yes	Yes	25, 43
F88	11,400	39.2	103.5	80	>24	Yes	Yes	30, 45
F127	12,600	65	100	70	22	Yes	Yes	27, 57

Abbreviations: HLB, hydrophilic–lipophilic balance; PEO, poly(ethylene oxide); PPO, poly(propylene oxide).

small molecules in the culture medium may partition into the oil phase, removing the essential nutrients required for cell viability. Nonetheless, the use of immiscible fillers is promising because some fluorinated liquids and silicone oils are biocompatible with endothelial cells and are used in vitreoretinal surgery (33). In addition, silicone oil has been used in cell (34) and embryo (35) culture systems to prevent evaporation and preserve sterility. Accordingly, several groups (26, 27, 36, 37) have used silicone oil for cell-based applications in DMF without reported toxicity (although no specific studies have been done to verify these effects).

The primary biocompatibility concerns for DMF cell culture are the potential effects on cell health of the applied electric field and the potential current flow that is associated with droplet manipulation. In a typical DMF system, a direct current (DC) or low-frequency alternating current (AC) voltage in the range of 80–140 V_{rms} is applied to the actuation electrodes. Since the electrodes are insulated by a dielectric layer, and cell-culture medium is conductive, the electric fields in the droplets are very weak (38). Indeed, according to numerical simulations (39), the voltage drop across a droplet on a device with standard dimensions is in range of nanovolts (10^{-9} V) for an applied voltage of 100 V DC. Similarly, because of the insulated electrodes, the current flowing through the device is often quite low (40). However, this should be verified on a case-by-case basis because the current flowing through the device is highly dependent on the operating conditions. In particular, the current in a device is affected by the driving voltage, the driving frequency, and the area of the electrode that is covered by a droplet (41). Consequently, a combination of high voltage, high frequency, and large electrode area may be sufficient to induce heating, as has been reported for the related technique of liquid dielectrophoresis (38). Nevertheless, using normal operating conditions, many researchers (26, 30, 36, 39, 42–44) have used live/dead assays to determine that DMF actuation does not affect apparent cell viability. In addition, algae, bacteria, yeast, and mammalian cells have been cultured in DMF systems and found to have similar proliferation rates when compared with macroscale culture systems (39, 42).

Although viability and proliferation assays are a useful first step, they are fairly crude end-point indicators of cell health and fitness. A more comprehensive analysis was carried out by Au et al. (45), who used cells expressing stress reporters tagged with green fluorescent protein, single-cell comet assays for DNA damage, and DNA microarrays for transcriptional profiling to test for

subtle effects on cell health in DMF devices. To establish the boundaries of the system, a range of different operating conditions were evaluated that varied the driving voltage and frequency, electrode size, and actuation time. Most DMF operating conditions tested, including those that have been commonly reported in the literature, resulted in negligible effects on cell stress or transcription. However, for devices operated using a combination of high driving frequency (18 kHz), large driving electrodes (10 mm × 10 mm), and long actuation time (15 minutes), significant damage to DNA integrity and differential transcriptional regulation were observed. Interestingly, for this detrimental (and atypical) condition, the authors observed significant heating in the droplet, with temperatures up to 56°C. Thus, to ensure the biocompatibility of DMF for cell-based applications, the authors recommended using standard conditions, including modest driving frequencies (≤10 kHz) and electrode sizes (≤5 mm). **Table 2** summarizes the DMF operating conditions that have been reported to be compatible with particular cells and organisms.

There is no evidence to suggest that DMF actuation under normal conditions is detrimental to cell health. However, any untested cell type should be evaluated against conventional macroscale formats to ensure that similar phenotypes are maintained; the breadth and depth of such assessments will depend on the application.

3. TYPES OF CELL CULTURE

Traditional cell-culture methods rely on cell-culture flasks and microtiter well plates. When robotic handlers are not available, reagents and cell suspensions must be individually pipetted, which is time consuming and labor intensive. In addition, these formats require relatively large volumes of reagents, which can impose a limit on the number of experiments that can be performed. DMF has the potential to address these and other challenges commonly encountered in traditional cell-culture methods. In this section, we discuss cell-culture implementations in DMF, including suspension cultures, two-dimensional (2D) cultures on planar substrates, and three-dimensional (3D) cultures in hydrogels.

3.1. Suspension Culture

DMF is, at heart, a technique that is used to manipulate droplets of liquid, so it is well suited for cells that grow while suspended in liquid culture medium. Hence, no modification is required to manipulate suspended mammalian cells and other microorganisms that are commonly cultured in suspension (e.g., bacteria, algae, yeast). As described in Section 4.1, cells suspended inside droplets may be further sorted or manipulated by the use of electrical, optical, or magnetic forces.

The first demonstration of mammalian suspension-cell manipulation in DMF was reported by Zhou et al. (36). Using a silicone-oil-filled device, the authors demonstrated that droplets containing human fetal osteoblast suspensions could be moved for 2 hours at 60 V without any observable effects on cell viability. The first mammalian cell-based assay implemented by DMF was demonstrated by Barbulovic-Nad et al. (39). With the help of a Pluronic additive, the authors carried out a toxicology-screening assay, in which droplets carrying Jurkat T cells were merged with droplets containing different concentrations of Tween 20, which is lethal to cells, and these droplets were then merged again with droplets carrying viability dyes to generate dose–response curves. The DMF assay was not only more sensitive than an identical one performed in a 384-well plate but it also reduced reagent consumption by 30-fold.

In a more recent example, Park et al. (46) exploited the versatility of DMF to characterize various cryoprotective agent mixtures. In this work, the authors used DMF to prepare droplets containing various ratios of dimethyl sulfoxide (DMSO) to phosphate-buffered saline (PBS) in

Table 2 Summary of digital microfluidic cell-culture operating parameters reported in the literature, by cell or organism

Cell or organism	Serum or protein in media, maximum concentration (%)	Antifouling reagent,[a] concentration (% weight/volume)	Maximum voltage (V_{rms})	Maximum frequency (kHz)	Maximum electrode area (mm^2)	Dielectric layer, thickness (μm)	Hydrophobic coating,[b] thickness (nm)	Reference
HepG2, NIH-3T3 (mammalian cell lines)	FBS, 8; CS, 2	Pluronic F88, 0.06	78	5	17	Parylene C, 6.9	Teflon AF, 235	30
Ba/F3 WeHi-3B (mammalian cell lines)	FBS, 10	Pluronic F88, 0.06	230	18	100	Parylene C, 6.9	Teflon AF, 235	45
Escherichia coli strain DH5α (bacteria), *Saccharomyces cerevisiae* strain BY4741 (yeast), *Cyclotellacryptica* (algae)	Yeast extract/tryptone/peptone/biotin/cyanocobalamin (maximum concentration not stated)	Pluronic F68, 0.1; F68, 0.02	177	5	100	Parylene C, 6.9	Teflon AF, 235	42
CHO-K1, NIH-3T3, HeLa and INS-1 (mammalian cell lines)	FBS, 10	Pluronic F68, 0.05	100	15	25	Parylene C, 2.5	Teflon AF, 50	49
Jurkat T (mammalian cell line)	FBS, 10	Pluronic F68, 0.2	140	15	50	Parylene C, 2	Teflon AF, 50	39
HeLa (mammalian cell line)	FBS, 10	Pluronic F68, 0.05	88	15	33	Parylene C, 7	Teflon AF, 50	66
MDCK (mammalian cell line)	FBS, 10	Pluronic F127, 0.02; F68, 0.02	140	10	5	Parylene C, 8	Teflon AF, 200	57
MDCK (mammalian cell line)	FBS, 10	Pluronic F68, 0.02	300	18	5	Parylene C, 8	Teflon AF, 200	51
Neuro-2a (mammalian cell line)	FBS, 7.5; HS, 7.5	Silicone-oil-filled	80	1	1	SU-8, 5	Teflon AF, 50	37
NIH-3T3 (mammalian cell line)	FBS, 10	Pluronic F68, 0.05; P105, 0.02	88	18	4	Parylene C, 15	Teflon AF, 200	43
Tetrahymena (protozoa)	Yeast extract/peptone	None	233	18	0.6	Candle soot, 30	Teflon AF	15
Arabidopsis thaliana protoplasts (primary plant cells)	None	None	130	1	8	Parylene C, 3	Teflon AF, 200	68
ICR mouse embryos (primary cell culture)	Amino acids	Pluronic F127, 0.08	52	Not stated	Not stated	SU-8, 1	Teflon AF, 55	27
MCF-7 (mammalian cell line)	FBS, 5	Pluronic F68, 0.2	100	1	1	SU-8, 1	Teflon AF, 250	46
HeLa (mammalian cell line)	Not stated	Pluronic F68, 0.2	120	20	Not stated	Silicon nitride, 1	Cytop, 1,000	63

(*Continued*)

Table 2 (*Continued*)

Cell or organism	Serum or protein in media, maximum concentration (%)	Antifouling reagent,[a] concentration (% weight/volume)	Maximum voltage (V_{rms})	Maximum frequency (kHz)	Maximum electrode area (mm^2)	Dielectric layer, thickness (μm)	Hydrophobic coating,[b] thickness (nm)	Reference
Human lymphocytes (primary cell culture)	AB human serum, 10	Tween 20, 0.015	80	1	1	Silicon nitride, 1	Cytop, 1,000	65
NIH-3T3, CHO-K1, HeLa (mammalian cell line)	FBS, 10	Pluronic F68, 0.05	120	15	35	Parylene C, 2	Teflon AF, 50	55
Cyclotella cryptica (algae)	Biotin/cyanocobalamin	Pluronic F68, 0.02	120	15	320	Parylene C, 7	Teflon AF, 50	69
Saccharomyces cerevisiae (yeast) and *Danio rerio* embryo (zebrafish)	None	None	105	8	50	Not stated	Not stated	47
Porcine aorta endothelial, valvular endothelial, and valvular interstitial cells (primary cell culture)	FBS, 10	Pluronic F68, 0.02	280	18	16	Parylene C, 7	Teflon AF, 200	70
HeLa (mammalian cell line)	Not stated	Pluronic F68, 0.2	14	10	Virtual	Hydrogenated amorphous silicon, 1 and aluminum oxide, 0.1 μm	Teflon AF, 25	64
MCF-7 (mammalian cell line)	Not stated	Silicone-oil core-shell plus Pluronic (identity and concentration not reported)	Not stated	Not stated	2.0	Parylene C, 2.8	Teflon AF, 300	26
HeLa (mammalian cell line)	FBS, 10	Pluronic F68, 0.1	130	7	2.0	Parylene C, 3	Teflon AF, 200	44
hFOBs 1.19 (mammalian cell line)	Not stated	Silicone-oil-filled	60	DC	0.6	Parylene C	Teflon AF	36

Abbreviations: CS, calf serum; FBS, fetal bovine serum; HS, horse serum.

[a]Pluronic (BASF, Ludwigshafen, Germany); Tween 20 (Croda International, Goole, UK).

[b]Teflon AF (DuPont, Wilmington, DE); Cytop (Asahi Glass, Tokyo, Japan).

mixtures with or without cells. After subjecting the droplets to freezing and thawing, the droplets were further mixed with dyes (Hoechst and propidium iodide) to assess post-thaw viability. In an example of a multicellular model, Li et al. (27) used DMF to manipulate mouse embryos. After on-chip culturing for 72 hours, the authors observed that the rate of blastocyst formation was similar to that of embryos cultivated in petri dishes.

The first demonstration of DMF for applications involving nonmammalian cells was reported by Son & Garrell (47). The authors used DMF to move yeast cells (*Saccharomyces cerevisiae*) and zebrafish embryos (*Danio rerio*) suspended in droplets. Not only did both organisms remain viable after transport, they were also able to develop normally after being removed from the device (**Figure 2*a*,*b***). Furthermore, the authors demonstrated the ability to perform on-chip dechorionation by mixing a droplet of digestive reagent with a droplet containing the embryo. Longer periods of microorganism culture were demonstrated by Au et al. (42), who developed a DMF-based microscale bioreactor for culturing bacteria, algae, and yeast. These microorganisms were grown in droplets on-chip for up to 5 days, with automated, semicontinuous mixing and temperature control. Cell densities were determined by measuring absorbances through transparent regions of the devices (**Figure 2*c***, *left*). Growth profiles generated in the DMF device were comparable to those generated in macroscale systems (**Figure 2*c***, *right*). As a proof of principle, the authors carried out a toxicity screen on yeast cells and performed bacterial transformation with a fluorescent reporter gene. Very recently (48), a "droplet-to-digital" platform was developed in which individual yeast cells were isolated into droplets in microchannels, followed by delivery to a DMF platform for long-term culture and metabolite production.

3.2. Two-Dimensional Culture

Most mammalian cell types, with the exception of blood cells and a few others, are adherent—that is, they require a suitable surface for attachment and proliferation. Despite this fact, the culturing of adherent cells has only recently been implemented in DMF systems, the first being reported in 2010 (49). One reason for this is the requirement that the device's architecture must be modified because the hydrophobic coatings used in DMF are incompatible with cell attachment and growth. To address this challenge, several patternable surface-modification techniques have been developed for performing adherent cell culture in DMF, including protein spotting, stenciled plasma etching and liftoff, and fluorocarbon liftoff.

The most straightforward method for forming patterns favorable for adherent cell growth is to spot extracellular matrix proteins (50) onto the hydrophobic surface of the device. This method was used by Barbulovic-Nad et al. (49) to develop a DMF platform capable of implementing all of the steps required for adherent mammalian cell culture and passaging: cell seeding, growth, detachment, and reseeding on a fresh surface. The adhesion pads were formed by spotting fibronectin solutions on the bottom plate of the DMF device using a pipette. The introduction of adhesion pads resulted in a useful fluidic phenomenon, termed passive dispensing. In passive dispensing, as a droplet is translated (on a surface that is primarily hydrophobic) across a hydrophilic site, a portion of the droplet is pinned to the pad, forming a subdroplet. This technique has been exploited to seed cells, exchange media on cells grown on adhesion pads, deliver reagents to detach cells, and transport a portion of the detached cells to a new adhesion pad for subculture. Using this approach, various immortalized cell lines (CHO-K1, NIH-3T3, HeLa, and INS-1) were cultured in multiple passages for up to 2 weeks, and had proliferation rates comparable to those found using conventional tissue-culture methods.

The manual spotting of protein onto unpatterned Teflon AF was a useful first step in developing adherent cell cultures, but the spots that are produced in this manner are relatively

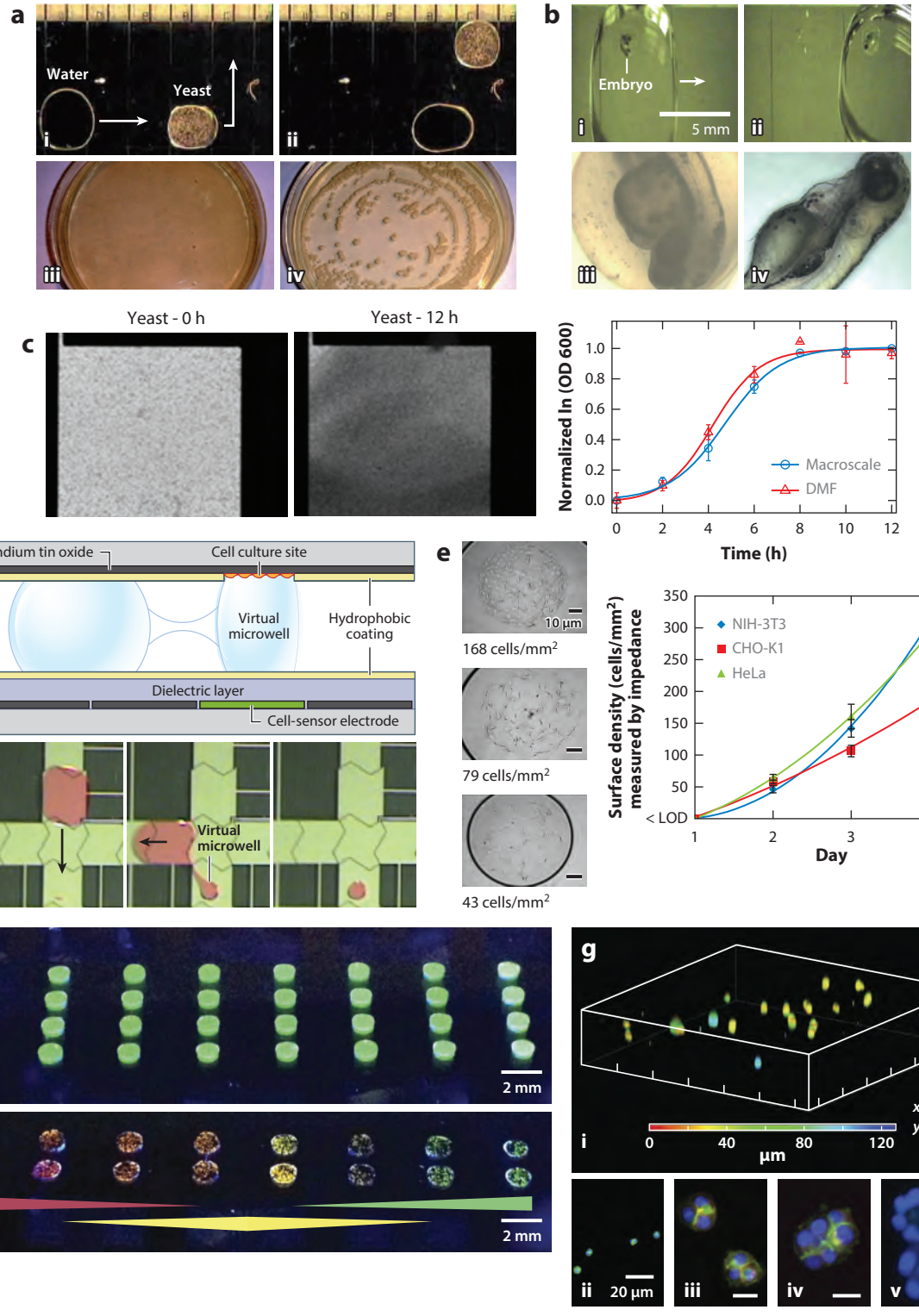
a
Water
Yeast
i
ii
iii
iv
b
Embryo
5 mm
i
ii
iii
iv
c
Yeast - 0 h
Yeast - 12 h
Normalized ln (OD 600)
1.0
0.8
0.6
0.4
0.2
0.0
0
2
4
6
8
10
12
Time (h)
Macroscale
DMF
d
Indium tin oxide
Cell culture site
Virtual microwell
Hydrophobic coating
Dielectric layer
Cell-sensor electrode
Virtual microwell
e
10 µm
168 cells/mm2
79 cells/mm2
43 cells/mm2
Surface density (cells/mm2) measured by impedance
350
300
250
200
150
100
50
< LOD
1
2
3
4
Day
NIH-3T3
CHO-K1
HeLa
f
i
2 mm
ii
2 mm
g
i
0
40
80
120
µm
z
x
y
ii
20 µm
iii
iv
v

large (1 × 1 mm) and suffer from irreproducible size, shape, and density (50, 51). To generate more precise adhesion pads, Witters et al. (44) developed a microfabrication technique that relies on plasma etching through a photoresist stencil followed by liftoff. Briefly, this technique comprises five steps: (*a*) a sacrificial Parylene layer is deposited on the bottom plate (on top of the Teflon AF coating); (*b*) photolithography is used to cover the device with photoresist except for the regions where adhesion pads are desired, and the exposed regions are etched to remove the underlying Teflon AF and Parylene C; (*c*) the photoresist is removed; (*d*) adhesion-promoting peptides (in this case, poly-L-lysine, PLL) are incubated on the device; and (*e*) the sacrificial Parylene C is peeled off. This fabrication technique allowed for HeLa cells to be arrayed as clusters on 40 μm diameter pads or as single cells on 15 μm diameter pads. Using the same technique, Vergauwe et al. (26) fabricated circular patches (250 μm diameter) of poly-L-lysine for on-chip seeding and culture of MCF-7 cells, which were cultured for up to 3 days.

In the surface-modification methods described above, the adhesion pads are formed on the bottom plate. From a practical standpoint, this format complicates the device-fabrication process and runs the risk of compromising the integrity of the hydrophobic coating (44) or the dielectric layer, or both. To circumvent this challenge, Eydelnant et al. (51) developed a fluorocarbon liftoff method for the top plate similar to the one described previously by Malic et al. (52) for other applications. This method can be used to form exposed, micron-dimension windows of bare ITO on an otherwise Teflon AF-coated surface. Briefly, the method comprises three steps: (*a*) using photolithography, islands of photoresist are patterned on an ITO substrate; (*b*) Teflon AF is spin-coated onto the substrate and then baked; and (*c*) the buried photoresist undergoes liftoff in acetone, and the substrate is then baked. Devices formed using the top-plate liftoff technique are suitable for cell culture without the addition of biomolecules or proteins (53). But because the sites are located on the top plate, the subdroplets generated by passive dispensing, termed virtual microwells, can be flexibly positioned over the array of driving electrodes without interfering with bottom-plate fabrication or geometry. Using this technique, Eydelnant et al. (51) demonstrated robust

Figure 2

(*a–c*) Suspension, (*d*,*e*) 2D adherent, and (*f*,*g*) 3D hydrogel cell culture demonstrated in digital microfluidic (DMF) systems. (*a*, *top*) Frames from a video (*i*, *ii*) depicting a water-collection droplet following the path of a droplet containing 2.8×10^5 yeast cells per mL. The water droplet collects residue or cells left behind by the moving yeast droplet. (*a*, *bottom*) After 4 days of culture: pictures of culture plates seeded with (*iii*) the contents of a collection droplet and (*iv*) a yeast droplet. Panel *a* modified from Reference 47 with permission from The Royal Society of Chemistry. (*b*, *top*) Frames from a video (*i*, *ii*) depicting a moving droplet containing a zebrafish embryo. (*b*, *bottom*) Pictures of the embryo (*iii*) 48 h after transport and (*iv*) after hatching. Panel *b* modified from Reference 47 with permission from The Royal Society of Chemistry. (*c*, *left*) Pictures of yeast cultured in a DMF microbioreactor after 0 and 12 h of incubation on the device. (*c*, *right*) Time series plot comparing yeast grown in macroscale (*blue circles*) or in the DMF bioreactor (*red triangles*). Optical density (OD) measurements were taken at 600 nm, and the natural log (ln) of these values was normalized to the highest value. Panel *c* modified from Reference 42 with permission from Springer. (*d*, *top*) Side-view schematic of a DMF device for cell culture and impedance sensing. (*d*, *bottom*, *left to right*) Frames from a video depicting the manipulation of a unit droplet (~1 μL) over a hydrophilic site such that it forms a virtual microwell (~0.2 μL) via passive dispensing. (*e*, *left*) Pictures of NIH-3T3 cells seeded at three different volumetric densities in virtual microwells, with surface densities listed under each picture. (*e*, *right*) Plot of cell surface densities for NIH-3T3 (*blue diamonds*), CHO-K1 (*red squares*), and HeLa cells (*green triangles*) measured by impedance as a function of time for 4 days. Abbreviation: LOD, limit of detection. Panel *e* modified from Reference 42 with permission from Elsevier. (*f*, *i*) Picture of a 32-plex array of microgels formed from Geltrex (Life Technologies, Carlsbad, CA) (containing fluorescein for visualization). (*f*, *ii*) Picture of a combinatorial array of Geltrex microgels containing mixtures of red, yellow, and/or green microspheres. Gradient bars indicate the percentage composition of each respective microsphere, from 100% red at the left to 100% green at the right. (*g*, *top*) Confocal microscopy image stack of (*i*) MDCK cells in a Geltrex microgel on a DMF device demonstrating cell distribution throughout the *z* axis. (*g*, *bottom*) Images depicting MDCK spheroid formation in a microgel on a DMF device (*ii*, day 1; *iii*, day 2; *iv*, day 3; *v*, day 4). Cells were stained for actin with phalloidin (*green*) and nuclei with Hoechst (*blue*). On day 4, lumen formation was observed. Panel *g* modified from Reference 57 with permission from Nature Publishing Group.

monolayer cell culture of MDCK and HeLa cell lines that had similar morphology and growth rates relative to cells grown on well plates. Further, in a direct comparison with the bottom-plate protein-spotting method (described above), the top-plate liftoff spots are superior to bottom-plate fibronectin adhesion pads in terms of cell attachment and reproducibility. Ng et al. (54) recently used top-plate fluorocarbon liftoff spots as an integral part of a new method called DISC, or digital microfluidic immunocytochemistry in single cells. DISC was used to evaluate receptor-mediated cell-signaling processes in >100,000 individual cells, at much higher time resolution (e.g., with 3-s pulses of stimulant) than is possible for conventional methods.

The fluorocarbon liftoff technique described above, in which cells adhere and proliferate on exposed ITO, is particularly useful because the ITO is conductive, and can be used for electrical sensing. Shih et al. (55) developed an impedance-sensing method for measuring the density of adherent cells grown in virtual microwells on top plates (**Figure 2*d***), with limits of detection of approximately 20–25 cells/mm^2. To validate this technique, the authors tracked the growth of three cell types (NIH-3T3, HeLa, and CHO-K1) for 4 days (**Figure 2*e***) and investigated the effects of culturing cells in serum-starved conditions. With a nearly 1,000-fold reduction in reagent use relative to commercial alternatives and with smart droplet control (56), this cell platform couples long-term cell culture with label-free sensing, and may be useful for a wide range of assays that use the cell-proliferation rate as a readout (e.g., toxicity screening).

3.3. Three-Dimensional Culture

Although 2D cell culture is still the method of choice for research laboratories and the pharmaceutical industry, cell culture in 3D is quickly gaining popularity because it has the potential to better recapitulate in vivo environments. The concept of 3D cell culture in DMF was first demonstrated by Fiddes et al. (43), who cultured NIH-3T3 cells in hydrogel discs for up to 7 days. To form each hydrogel disc, a mixture of sol-phase agarose and cell suspension was pipetted onto the bottom plate of a DMF device. Upon assembling the top plate, the sol-phase mixture was subjected to cold temperature (near 4°C) to facilitate gelation of the agarose. The resulting discs (containing cells) were held in place by the adhesion and static friction forces of the top and bottom plates, which facilitated media and reagent exchange by passive dispensing. Building on this method, Eydelnant et al. (57) used virtual microwells and passive dispensing to achieve microgel formation on demand. To form each microgel, a mixture of sol-phase Geltrex (Life Technologies, Carlsbad, CA) and MDCK cell suspension (at 4°C) is transported across a hydrophilic site, forming a passively dispensed virtual microwell. As the temperature is increased, the sol-phase subdroplet crosslinks to form a pillar-shaped hydrogel. This technique is automated and versatile, allowing the formation of gels of different shapes or matrix composition, or both, as well as arrays of combinatorial gels with varying mixtures of matrix or cells (**Figure 2*f***). Using this method, MDCK cells can be seeded with high viability (>80%) throughout each microgel in the *z* axis (**Figure 2*g***, *top*). After 4 days of culture, hollow spheroids can be observed (**Figure 2*g***, *bottom*), recapitulating 3D growth morphology. Unlike traditional liquid-handling methods (i.e., manual or robotic pipetting in 96-well plates), DMF manipulation of cells in hydrogel pillars was found to be particularly gentle: The spheroid structure remains intact during washing and reagent exchange. Free-floating 3D cell constructs (not constricted to pillars) have also recently been demonstrated to be compatible with DMF (30, 58), as well as methods for forming chemically crosslinked hydrogels for 3D cell culture (59). These examples suggest that DMF may be a useful platform for automated development and screening of 3D-engineered tissues.

4. CELL-BASED APPLICATIONS

Because DMF cell culture is still a relatively nascent field, the number of true cellular applications in DMF is limited. As described in the preceding sections, most work has focused on establishing device biocompatibility or demonstrating proofs of principle. In this section, we discuss the most mature examples of DMF cell-based applications, which fall into three broad categories: cell sorting, toxicity screens, and functional assays.

4.1. Cell Sorting

Cell purification and sorting are critical steps in assays that study a specific subpopulation of cells. Electrical, optical, and magnetically induced forces have been employed in DMF devices to manipulate and sort cells within droplets. As an example of the method of using electrical forces, Fan et al. (37) used dielectrophoresis (DEP) to manipulate neuroblastoma cells inside a droplet. By applying the appropriate voltage and frequency (up to 2 MHz), DEP forces were generated, causing cells to accumulate preferentially in one side of a droplet. The droplet was then split into two subdroplets such that one subdroplet contained a mixture of cells at high density. Other electrically driven methods used for sorting particles in droplets in DMF include electrophoresis (60), traveling-wave dielectrophoresis (61), and negative dielectrophoresis (62).

Shah et al. (63) provided an example of using optical forces to sort cells in droplets manipulated by DMF. These authors developed an integrated DMF lateral-field optoelectronic tweezer device. When an optical pattern is projected onto a photoconductive layer, cells can be manipulated by the optoelectronic tweezer effect. Using this technique, the authors concentrated HeLa cells on one side of a droplet, allowing for the generation of a high-density subdroplet, similar to the DEP application described by Fan et al. (37). In related work, Valley et al. (64) developed a unified optoelectronic platform that can simultaneously actuate droplets and manipulate particles within droplets using light (i.e., optoelectrowetting and optoelectronic tweezers). Remarkably, the authors were able to select a single HeLa cell of interest from a population of cells and isolate it into its own subdroplet (**Figure 3*a***).

Shah et al. (65) provided an example of using magnetic forces to manipulate cells within droplets on DMF devices. These authors developed a system in which a droplet containing anti-CD8-conjugated magnetic beads was merged with a droplet containing a mixture of $CD8^+$ and $CD8^-$ T lymphocyte cells. In the pooled droplet, the $CD8^+$ cells selectively bound to the magnetic beads and an external magnet was used to purify these cells from the unbound cells. Using this technique, the authors demonstrated that the $CD8^+$ cells bind very efficiently to the beads (approximately 92% were bound) and that 35% of the $CD8^-$ cells can be depleted in one step. It is likely that even higher depletion rates may be possible if this process is coupled with more efficient washing procedures (32). This method of cell purification is particularly attractive because it is straightforward to implement and can be used to collect any cell type that can be tagged with an antibody. Since magnetic-bead cell purification is commonly performed in the macroscale, many commercial sources of beads and antibodies are available.

4.2. Toxicity Screens

Cell-viability assays, in the form of staining with calcein AM (to identify live cells) and ethidium homodimer-1 or propidium iodide (to identify dead cells), are the assays most commonly performed using DMF (26, 30, 36, 39, 42–44, 46). However, these are nonspecific assays that rely

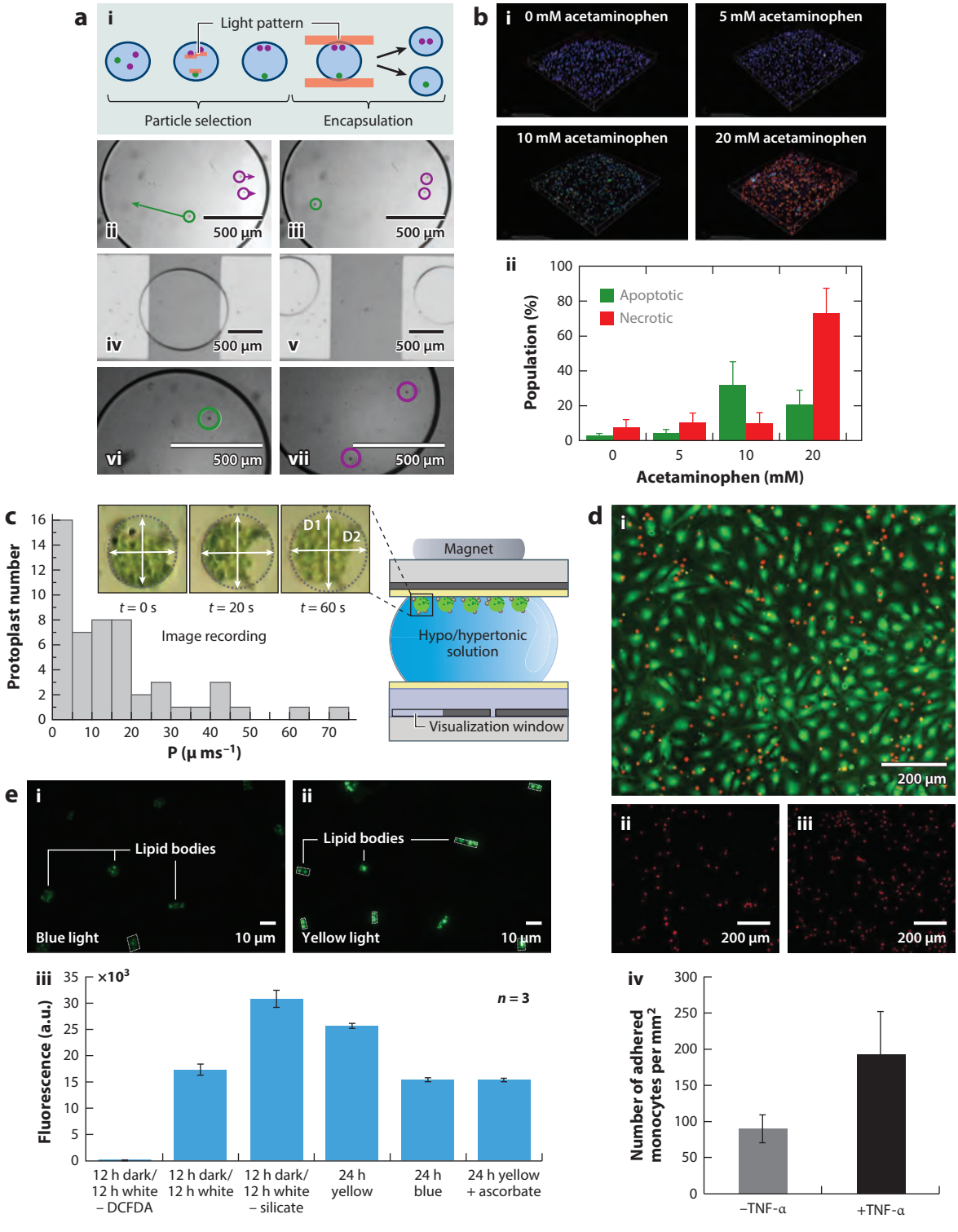
a
i
Light pattern
Particle selection
Encapsulation
ii
500 µm
iii
500 µm
iv
500 µm
v
500 µm
vi
500 µm
vii
500 µm
b
i
0 mM acetaminophen
5 mM acetaminophen
10 mM acetaminophen
20 mM acetaminophen
ii
Apoptotic
Necrotic
Population (%)
Acetaminophen (mM)
c
Protoplast number
P (µ ms−1)
t = 0 s
t = 20 s
t = 60 s
D1
D2
Image recording
Magnet
Hypo/hypertonic solution
Visualization window
d
i
200 µm
ii
200 µm
iii
200 µm
e
i
Lipid bodies
Blue light
10 µm
ii
Lipid bodies
Yellow light
10 µm
iii
×10³
n = 3
Fluorescence (a.u.)
12 h dark/ 12 h white – DCFDA
12 h dark/ 12 h white
12 h dark/ 12 h white – silicate
24 h yellow
24 h blue
24 h yellow + ascorbate
iv
Number of adhered monocytes per mm²
–TNF-α
+TNF-α

either on intracellular enzymatic activity (e.g., esterase) or membrane-integrity status. Thus, any cytotoxic events that do not affect these properties may not be detected. Extending on these simple viability assays, Bogojevic et al. (66) developed a DMF method for evaluating apoptosis. This was implemented using a fluorogenic substrate for caspase-3, an apoptosis marker that is a popular target for the discovery of anticancer drugs. Using DMF and virtual microwells, the authors seeded and cultured HeLa cells in parallel chambers overnight, then incubated the cells with various doses of cytotoxic agents (e.g., staurosporine), and determined the degree of apoptosis induction via caspase-3 activity. Interestingly, in a direct comparison with an equivalent well-plate method, the DMF approach had better sensitivity and dynamic range mainly because DMF manipulation is gentler than pipetting (i.e., in DMF there is less cell delamination). This work demonstrated that parallel assays of the type commonly used in the pharmaceutical industry can be performed on a DMF device.

Often, drugs that seem promising when tested on adherent (2D) cells fail when tested in animal models. To meet the need for a better screening method for drug toxicity, Au et al. (30) developed a DMF-based method to screen for hepatotoxicity in 3D self-assembled spheroid aggregates (also known as organoids). These individually addressable free-floating tissue constructs were formed on-chip by mixing two cell lines, HepG2 and NIH-3T3 in collagen hydrogels. To facilitate the exchange of reagent and media, the authors fabricated SU-8 pillars [building on filtering work described previously (67)] on the bottom plate of the device to confine the organoids to predetermined locations. To evaluate the liver-like functionality of the organoids, they were assessed for viability and albumin production during a 4-day period. Subsequently, the organoids were employed in two proof-of-principle drug-screening assays. The first was a cytochrome P450 induction assay in which the liver organoids were incubated with dexamethasone to induce the

Figure 3

Applications of cell culture in digital microfluidic (DMF) systems, including (*a*) cell sorting, (*b*) toxicity screening, and (*c–e*) functional assays. (*a*, *i*) Diagram depicting, first, optical forces used to sort two cells into two categories (*purple* and *green*) on opposite sides of a droplet; second, depiction of the droplet split into two subdroplets. Images depicting (*a*, *ii*,*iii*) the first and (*a*, *iv*,*v*) second processes, and (*a*, *vi*,*vii*) close-up images of the final subdroplets containing the cells. Panel *a* modified from Reference 64 with permission from The Royal Society of Chemistry. (*b*) Hepatotoxicity assay using DMF. Confocal images of (*b*, *i*) hepatic organoids exposed to increasing concentrations of acetaminophen, stained for total nuclei using Hoechst 33342 (*blue*) and apoptotic cells using NucView488 (Biotium, Hayward, CA) (*green*) or necrotic cells using ethidium homodimer-1 (*red*). (*b*, *ii*) Plot of percentage of the cell population in apoptotic (*green*) or necrotic (*red*) state as functions of acetaminophen concentration. The percentage of cells that are apoptotic peaks at 10 mM acetaminophen and then switches to necrosis at higher concentrations. Panel *b* modified from Reference 30 with permission from The Royal Society of Chemistry. (*c*) Measurement of the effects of osmotic pressure changes in individual plant protoplasts. (*c*, *left*) Histogram of protoplast distribution as a function of the permeability coefficient (P); (*c*, *center*) images of protoplast at time $t = 0$, 20, and 60 s after exchange into hypotonic buffer (with measurements of diameters D1 and D2); and (*c*, *right*) diagram depicting orientation of individual protoplasts held in position by magnetic forces. Panel *c* modified from Reference 68 with permission from Elsevier. (*d*) Monocyte attachment to primary endothelial cells. (*d*, *i*) Fluorescence image of adherent endothelial cells [stained with calcein AM (*green*)] that were subsequently incubated with Hoechst 33342-labeled THP-1 monocytes (*red*) on-device. Fluorescence images of labeled monocytes (*red*) in this system (*d*, *ii*) after incubation of endothelial cells with control or (*d*, *iii*) after stimulation of endothelial cells with tumor necrosis factor-α (TNF-α). (*d*, *iv*) Plot of number of monocytes adhered to endothelial cells after (*left*) incubation with control or (*right*) stimulation. Panel *d* modified from Reference 70 with permission from The Royal Society of Chemistry. (*e*) Lipid production in algae. Fluorescent images of algae cells grown on a DMF platform while incubated for 24 h under (*e*, *i*) blue or (*e*, *ii*) yellow light, with lipids stained with LipidTOX (Invitrogen, Carlsbad, CA) (*green*). (*e*, *iii*) Plot of dichlorofluorescein diacetate (DCFDA) fluorescence intensity (a reporter of oxidative stress) for (*left to right*): control (with no reporter), control (with reporter), algal cells exposed to silicate deprivation, algal cells cultured under yellow light, algal cells cultured under blue light, and algal cells cultured under yellow light with ascorbate (oxygen scavenger). As shown, algal cells cultured under yellow light have increased oxidative stress, suggesting a relationship between that stress and lipid accumulation. Abbreviation: a.u., arbitrary units. Panel *e* modified from Reference 69 with permission from The Royal Society of Chemistry.

expression of the cytochrome P450 isoform 3A4, with changes in enzyme activity measured using a fluorescent reporter. The authors observed that this effect could be detected only using the DMF device with 3D organoids and not in a 96-well plate format with 2D cells, suggesting that the assay is more sensitive in the DMF format. As shown in **Figure 3*b***, the second assay was for hepatotoxicity; in this assay organoids were incubated with increasing concentrations of acetaminophen (with the dilution series formed on-chip) for 24 hours, and cells were stained for apoptosis (using a caspase-3 activity reporter) and necrosis (using ethidium homodimer-1). This work, representing the first organ-on-a-chip DMF platform, illustrated the versatility of DMF platforms as a screening tool for liver function. If widely adopted, similar methods may be viable for drug development.

4.3. Functional Assays

There are a few recent examples of DMF being used to study cellular function in a range of organisms, including protoplasts from *Arabidopsis thaliana*, primary cells isolated from porcine aorta, and algae (*Cyclotella cryptica*). In the first example, Kumar et al. (68) developed a DMF assay to magnetically entrap individual protoplasts from *A. thaliana* to measure the osmotic potential of plasma membranes. After labeling the protoplasts with magnetic beads in tubes, the protoplasts were loaded onto the chip to measure water permeability. With the help of a magnet, individual protoplasts were held in place while DMF was used to wash the cells with a hypo- or hypertonic solution. During this process, the cells were imaged to determine the changes in the size of the protoplast. This proof-of-principle semiautomated DMF approach produced measurements of water permeability that are consistent with values in the literature (**Figure 3*c***). Furthermore, the DMF technique had a substantial increase in throughput (allowing for the manipulation and analysis of up to 7 protoplasts simultaneously) over traditional methods that measure only one protoplast at a time. This work also demonstrated the ability of DMF platforms to rapidly exchange buffers on cells grown in suspension, with low shear stress during live-cell imaging (69).

In the second example, Srigunapalan et al. (70) used DMF and virtual microwells to culture primary cells isolated from porcine aorta. Cells from three locations in the aorta (endothelial cells, valvular endothelial cells, and valvular interstitial cells) were cultured on-device for up to 1 week prior to implementing monocyte-adhesion assays. In these assays, endothelial cells that had been exposed to an inflammatory cytokine [tumor necrosis factor-α (TNF-α)] exhibited enhanced attachment to monocytes, which confirmed that primary cells cultured in this format maintained their in vivo-like phenotype (**Figure 3*d***). Since very small numbers of cells were needed for these assays, there was no need to perform cell expansion, a process that is particularly difficult and time consuming for sensitive slow-growing primary cells.

In the final example, Shih et al. (69) used a DMF platform to determine which conditions maximize nonpolar lipid generation in *C. cryptica*, an algae that has been proposed to be a useful candidate for biofuel production. While culturing the algae under different illumination conditions, the authors determined that different wavelengths of light affected both the proliferation rate and the amount of lipids produced. Specifically, blue light enhanced proliferation rates but resulted in low levels of lipid bodies in the cells, and yellow light resulted in reduced rates of proliferation but caused the generation of high levels of lipids, as shown by enlarged lipid bodies in the cells. Moreover, this lipid-accumulation effect under yellow light, which had not been reported previously, was found to correlate with increased oxidative stress (**Figure 3*e***). With the help of DMF, these informative screens were performed with minimal human intervention, using fewer

than 20 pipette steps compared with 600 pipette steps for a comparable manual assay. This work demonstrates the utility of DMF as an automated platform for multiplexed biological assays.

5. CONCLUSIONS AND FUTURE OUTLOOK

In this review, we have summarized the state of the art in DMF cell culture and analysis. In just 7 years since the first report of a DMF cell-based assay [in 2008 (39)], there have now been more than 25 peer-reviewed publications describing DMF devices used for applications related to cell and organism culture. During this period, critical design considerations, including nonspecific protein adsorption and biocompatibility, have been addressed. Likewise, proofs of principle have been demonstrated for DMF handling of cells grown in suspension, as 2D layers, and as 3D tissue-like constructs. Finally, the first applications have begun to emerge, including the ability to probe the effects of osmotic pressure in single protoplast cells and the determination of culture conditions favorable for lipid biosynthesis in algae. We are particularly enthusiastic about the use of DMF for applications involving hazardous reagents (e.g., toxins) or pathogens (e.g., Ebola virus) because the safety of such studies is vastly improved when they can be conducted using small volumes of reagents in isolated, automated systems.

Our enthusiasm for DMF cell culture does not, of course, mean that there are no challenges to be resolved. The technique is still in its infancy and is currently used in just a handful of labs around the world. For significant growth beyond these boundaries, challenges must be addressed, including improving methods for resisting the effects of biofouling (perhaps by using or developing more effective additives or fouling-resistant coatings), the fabrication of complex devices [which may be mitigated to some extent by printed electronic devices (71, 72)], and complicated electronic control systems [which may be mitigated to some extent by open-source software and hardware platforms (73)]. For the method to truly be useful to the life sciences community, an all-in-one integrated system must be developed to facilitate the control of humidity, temperature, and gas pressure.

Despite these challenges, we are optimistic about the future. The number of research groups using these techniques continues to grow, and the trajectory of advances during the past 7 years suggests there will be exciting new developments in the years to come. DMF offers unparalleled control over reagents, media, and cells, which suggests the possibility of interesting new studies that may not be possible using conventional techniques. DMF will certainly not solve all problems for all applications, but we propose that as the technology continues to evolve and mature, it may eventually become an important tool for research in the life sciences.

DISCLOSURE STATEMENT

The authors are not aware of any affiliations, memberships, funding, or financial holdings that might be perceived as affecting the objectivity of this review.

ACKNOWLEDGMENTS

We thank the Natural Sciences and Engineering Research Council of Canada (NSERC) for financial support. A.H.C.N. thanks NSERC for a graduate fellowship, and A.R.W. thanks the Canada Research Chair (CRC) Program for a CRC.

LITERATURE CITED

1. Chapman T. 2003. Lab automation and robotics: automation on the move. *Nature* 421:661–66
2. Sackmann EK, Fulton AL, Beebe DJ. 2014. The present and future role of microfluidics in biomedical research. *Nature* 507:181–89
3. Paul SM, Mytelka DS, Dunwiddie CT, Persinger CC, Munos BH, et al. 2010. How to improve R&D productivity: the pharmaceutical industry's grand challenge. *Nat. Rev. Drug Discov.* 9:203–14
4. Bhatia SN, Ingber DE. 2014. Microfluidic organs-on-chips. *Nat. Biotechnol.* 32:760–72
5. Mehling M, Tay S. 2014. Microfluidic cell culture. *Curr. Opin. Biotechnol.* 25:95–102
6. Squires TM, Quake SR. 2005. Microfluidics: fluid physics at the nanoliter scale. *Rev. Mod. Phys.* 77:977–1026
7. Fair RB, Khlystov A, Tailor TD, Ivanov V, Evans RD, et al. 2007. Chemical and biological applications of digital-microfluidic devices. *IEEE Des. Test. Comput.* 24:10–24
8. Choi K, Ng AHC, Fobel R, Wheeler AR. 2012. Digital microfluidics. *Annu. Rev. Anal. Chem.* 5:413–40
9. Malic L, Brassard D, Veres T, Tabrizian M. 2010. Integration and detection of biochemical assays in digital microfluidic LOC devices. *Lab Chip* 10:418–31
10. Cho SK, Moon H, Kim CJ. 2003. Creating, transporting, cutting, and merging liquid droplets by electrowetting-based actuation for digital microfluidic circuits. *J. Microelectromech. Syst.* 12:70–80
11. Absolom DR, Zingg W, Neumann AW. 1987. Protein adsorption to polymer particles: role of surface properties. *J. Biomed. Mater. Res.* 21:161–71
12. Norde W. 1986. Adsorption of proteins from solution at the solid–liquid interface. *Adv. Colloid Interface Sci.* 25:267–340
13. Luk VN, Mo GC, Wheeler AR. 2008. Pluronic additives: a solution to sticky problems in digital microfluidics. *Langmuir* 24:6382–89
14. Yoon JY, Garrell RL. 2003. Preventing biomolecular adsorption in electrowetting-based biofluidic chips. *Anal. Chem.* 75:5097–102
15. Freire SLS, Tanner B. 2013. Additive-free digital microfluidics. *Langmuir* 29:9024–30
16. Srinivasan V, Pamula VK, Fair RB. 2004. An integrated digital microfluidic lab-on-a-chip for clinical diagnostics on human physiological fluids. *Lab Chip* 4:310–15
17. Pollack MG, Pamula VK, Eckhardt AE, Srinivasan V. 2011. Protein crystallization screening and optimization droplet actuators, systems and methods. US Patent No. US8007739 B2
18. Ren H, Fair RB, Pollack MG, Shaughnessy EJ. 2002. Dynamics of electro-wetting droplet transport. *Sens. Actuators B: Chem.* 87:201–6
19. Brassard D, Malic L, Normandin F, Tabrizian M, Veres T. 2008. Water-oil core-shell droplets for electrowetting-based digital microfluidic devices. *Lab Chip* 8:1342–49
20. Fan S-K, Hsu Y-W, Chen C-H. 2011. Encapsulated droplets with metered and removable oil shells by electrowetting and dielectrophoresis. *Lab Chip* 11:2500–8
21. Aijian AP, Chatterjee D, Garrell RL. 2012. Fluorinated liquid-enabled protein handling and surfactant-aided crystallization for fully in situ digital microfluidic MALDI-MS analysis. *Lab Chip* 12:2552–59
22. Perry G, Coffinier Y, Boukherroub R, Thomy V. 2013. Investigation of the anti-biofouling properties of graphene oxide aqueous solutions by electrowetting characterization. *J. Mater. Chem. A* 1:12355–60
23. Perry G, Thomy V, Das MR, Coffinier Y, Boukherroub R. 2012. Inhibiting protein biofouling using graphene oxide in droplet-based microfluidic microsystems. *Lab Chip* 12:1601–4
24. Amiji M, Park K. 1992. Prevention of protein adsorption and platelet adhesion on surfaces by PEO/PPO/PEO triblock copolymers. *Biomaterials* 13:682–92
25. Au SH, Kumar P, Wheeler AR. 2011. A new angle on Pluronic additives: advancing droplets and understanding in digital microfluidics. *Langmuir* 27:8586–94
26. Vergauwe N, Witters D, Ceyssens F, Vermeir S, Verbruggen B, et al. 2011. A versatile electrowetting-based digital microfluidic platform for quantitative homogeneous and heterogeneous bio-assays. *J. Micromech. Microeng.* 21:054026
27. Li C-C, Hsu Y-W, Fan S-K, Huang H-Y. 2012. Dynamic embryo culture on a digital microfluidic chip. In *Nano/Molecular Medicine and Engineering*, pp. 74–77. New York: IEEE (Inst. Electr. Electron. Eng.)

28. Sarvothaman MK, Kim KS, Seale B, Brodersen PM, Walker GC, Wheeler AR. 2015. Dynamic fluoroalkyl polyethylene glycol co-polymers: a new strategy for reducing protein adhesion in lab-on-a-chip devices. *Adv. Funct. Mater.* 25:506–15
29. GE Healthc. Life Sci. 2014. *HyClone™ HyCell™ CHO Media.* Piscataway, NJ: GE Healthc. Life Sci., retrieved on September 11, 2014. **https://promo.gelifesciences.com/gl/hyclone/product/hyclone-hycell-cho-media.html**
30. Au SH, Chamberlain MD, Mahesh S, Sefton MV, Wheeler AR. 2014. Hepatic organoids for microfluidic drug screening. *Lab Chip* 14:3290–99
31. Wang K, Ruan J, Song H, Zhang J, Wo Y, et al. 2011. Biocompatibility of graphene oxide. *Nanoscale Res. Lett.* 6:8
32. Shah GJ, Kim CJ. 2009. Meniscus-assisted high-efficiency magnetic collection and separation for EWOD droplet microfluidics. *J. Microelectromech. Syst.* 18:363–75
33. Malchiodi-Albedi F, Morgillo A, Formisano G, Paradisi S, Perilli R, et al. 2002. Biocompatibility assessment of silicone oil and perfluorocarbon liquids used in retinal reattachment surgery in rat retinal cultures. *J. Biomed. Mater. Res.* 60:548–55
34. Luong-Van E, Kang RKC, Birch WR. 2009. A novel technique for positioning multiple cell types by liquid handling. *Biointerphases* 4:13–18
35. Pereira DC, Dode MAN, Rumpf R. 2005. Evaluation of different culture systems on the in vitro production of bovine embryos. *Theriogenology* 63:1131–41
36. Zhou J, Lu L, Byrapogu K, Wootton DM, Lelkes PI, Fair R. 2007. Electrowetting-based multi-microfluidics array printing of high resolution tissue construct with embedded cells and growth factors. *Virtual Phys. Prototyp.* 2:217–23
37. Fan SK, Huang PW, Wang TT, Peng YH. 2008. Cross-scale electric manipulations of cells and droplets by frequency-modulated dielectrophoresis and electrowetting. *Lab Chip* 8:1325–31
38. Jones TB, Fowler JD, Chang YS, Kim C-J. 2003. Frequency-based relationship of electrowetting and dielectrophoretic liquid microactuation. *Langmuir* 19:7646–51
39. Barbulovic-Nad I, Yang H, Park PS, Wheeler AR. 2008. Digital microfluidics for cell-based assays. *Lab Chip* 8:519–26
40. Fair RB. 2007. Digital microfluidics: Is a true lab-on-a-chip possible? *Microfluid. Nanofluid.* 3:245–81
41. Sadeghi S, Ding H, Shah GJ, Chen S, Keng PY, et al. 2012. On chip droplet characterization: a practical, high-sensitivity measurement of droplet impedance in digital microfluidics. *Anal. Chem.* 84:1915–23
42. Au SH, Shih SCC, Wheeler AR. 2011. Integrated microbioreactor for culture and analysis of bacteria, algae and yeast. *Biomed. Microdevices* 13:41–50
43. Fiddes LK, Luk VN, Au SH, Ng AHC, Luk V, et al. 2012. Hydrogel discs for digital microfluidics. *Biomicrofluidics* 6:014112
44. Witters D, Vergauwe N, Vermeir S, Ceyssens F, Liekens S, et al. 2011. Biofunctionalization of electrowetting-on-dielectric digital microfluidic chips for miniaturized cell-based applications. *Lab Chip* 11:2790–94
45. Au SH, Fobel R, Desai SP, Voldman J, Wheeler AR. 2013. Cellular bias on the microscale: probing the effects of digital microfluidic actuation on mammalian cell health, fitness and phenotype. *Integr. Biol.* 5:1014–25
46. Park S, Wijethunga PAL, Moon H, Han B. 2011. On-chip characterization of cryoprotective agent mixtures using an EWOD-based digital microfluidic device. *Lab Chip* 11:2212–21
47. Son SU, Garrell RL. 2009. Transport of live yeast and zebrafish embryo on a droplet ("digital") microfluidic platform. *Lab Chip* 9:2398–401
48. Shih SCC, Gach PC, Sustarich J, Simmons BA, Adams PD, et al. 2015. A droplet-to-digital (D2D) microfluidic device for single cell assays. *Lab Chip* 15:225–36
49. Barbulovic-Nad I, Au SH, Wheeler AR. 2010. A microfluidic platform for complete mammalian cell culture. *Lab Chip* 10:1536–42
50. Miller E, Ng AC, Uddayasankar U, Wheeler A. 2011. A digital microfluidic approach to heterogeneous immunoassays. *Anal. Bioanal. Chem.* 399:337–45
51. Eydelnant IA, Uddayasankar U, Li B, Liao MW, Wheeler AR. 2012. Virtual microwells for digital microfluidic reagent dispensing and cell culture. *Lab Chip* 12:750–57

52. Malic L, Veres T, Tabrizian M. 2009. Biochip functionalization using electrowetting-on-dielectric digital microfluidics for surface plasmon resonance imaging detection of DNA hybridization. *Biosens. Bioelectron.* 24:2218–24
53. Qiu Q, Sayer M, Kawaja M, Shen X, Davies JE. 1998. Attachment, morphology, and protein expression of rat marrow stromal cells cultured on charged substrate surfaces. *J. Biomed. Mater. Res.* 42:117–27
54. Ng AHC, Chamberlain MD, Situ H, Lee V, Wheeler AR. 2015. Digital microfluidic immunocytochemistry in single cells. *Nat. Commun.* 6:7513
55. Shih SCC, Barbulovic-Nad I, Yang X, Fobel R, Wheeler AR. 2013. Digital microfluidics with impedance sensing for integrated cell culture and analysis. *Biosens. Bioelectron.* 42:314–20
56. Shih SCC, Fobel R, Kumar P, Wheeler AR. 2011. A feedback control system for high-fidelity digital microfluidics. *Lab Chip* 11:535–40
57. Eydelnant IA, Lim BB, Wheeler AR. 2014. Microgels on-demand. *Nat. Commun.* 5:3355
58. Aijian AP, Garrell RL. 2015. Digital microfluidics for automated hanging drop cell spheroid culture. *J. Lab. Autom.* 20:283–95
59. George SM, Moon H. 2015. Digital microfluidic three-dimensional cell culture and chemical screening platform using alginate hydrogels. *Biomicrofluidics* 9:024116
60. Cho SK, Zhao Y, Kim CJ. 2007. Concentration and binary separation of micro particles for droplet-based digital microfluidics. *Lab Chip* 7:490–98
61. Zhao Y, Yi UC, Cho SK. 2007. Microparticle concentration and separation by traveling-wave dielectrophoresis (twDEP) for digital microfluidics. *J. Microelectromech. Syst.* 16:1472–81
62. Nejad HR, Chowdhury OZ, Buat MD, Hoorfar M. 2013. Characterization of the geometry of negative dielectrophoresis traps for particle immobilization in digital microfluidic platforms. *Lab Chip* 13:1823–30
63. Shah GJ, Ohta AT, Chiou EP, Wu MC, Kim CJ. 2009. EWOD-driven droplet microfluidic device integrated with optoelectronic tweezers as an automated platform for cellular isolation and analysis. *Lab Chip* 9:1732–39
64. Valley JK, Ningpei S, Jamshidi A, Hsu HY, Wu MC. 2011. A unified platform for optoelectrowetting and optoelectronic tweezers. *Lab Chip* 11:1292–97
65. Shah GJ, Veale JL, Korin Y, Reed EF, Gritsch HA, Kim CJ. 2010. Specific binding and magnetic concentration of CD8+ T-lymphocytes on electrowetting-on-dielectric platform. *Biomicrofluidics* 4:44106
66. Bogojevic D, Chamberlain MD, Barbulovic-Nad I, Wheeler AR. 2012. A digital microfluidic method for multiplexed cell-based apoptosis assays. *Lab Chip* 12:627–34
67. Schertzer MJ, Ben-Mrad R, Sullivan PE. 2011. Mechanical filtration of particles in electrowetting on dielectric devices. *J. Microelectromech. Syst.* 20:1010–15
68. Kumar PT, Toffalini F, Witters D, Vermeir S, Rolland F, et al. 2014. Digital microfluidic chip technology for water permeability measurements on single isolated plant protoplasts. *Sens. Actuators B: Chem.* 199:479–87
69. Shih SCC, Mufti NS, Chamberlain MD, Kim J, Wheeler AR. 2014. A droplet-based screen for wavelength-dependent lipid production in algae. *Energy Environ. Sci.* 7:2366–75
70. Srigunapalan S, Eydelnant IA, Simmons CA, Wheeler AR. 2012. A digital microfluidic platform for primary cell culture and analysis. *Lab Chip* 12:369–75
71. Fobel R, Kirby AE, Ng AHC, Farnood RR, Wheeler AR. 2014. Paper microfluidics goes digital. *Adv. Mater.* 26:2838–43
72. Ko H, Lee J, Kim Y, Lee B, Jung C-H, et al. 2014. Active digital microfluidic paper chips with inkjet-printed patterned electrodes. *Adv. Mater.* 26:2335–40
73. Fobel R, Fobel C, Wheeler AR. 2013. DropBot: an open-source digital microfluidic control system with precise control of electrostatic driving force and instantaneous drop velocity measurement. *Appl. Phys. Lett.* 102:193513